Modelling, Simulation and Characterization of a Supercapacitor in Automotive Applications

Vincenzo Castiglia, Nicola Campagna, *Student member, IEEE,* Antonino Oscar Di Tommaso, Rosario Miceli, *Member, IEEE,* Claudio Nevoloso, Filippo Pellitteri, Christian Puccio, and Fabio Viola
Department of Engineering
Palermo University
90128 Palermo, Italy
vincenzo.castiglia@unipa.it

***Abstract*—In the energy storage field, supercapacitors (SCs) are gaining more and more attention thanks to features such as high-power density, high life cycles and lack of maintenance. In this article, an improved SC three-branches model which considers the residual charge phenomenon is presented. The procedure to estimate the model parameters and the related experimental set-up are presented. The parameter estimation procedure is repeated for several SCs of the same type. The average parameters are then obtained and used as initial guesses for a recursive least square optimization algorithm, to increase the accuracy of the model. The model of a single SC is then extended to SC banks, testing different configurations and operating conditions. The simulation results, obtained in Matlab/Simulink environment for both the single SC and the different SC bank configurations, are validated with experimental tests to assess the model accuracy.**

***Index Terms*—supercapacitor (SC), modelling, energy storage, parameter estimation.**

I. Introduction

TRANSITIONING to sustainable, green transportation, together with the constant growth of renewable energy source generation plants, is essential to decrease air pollution and CO_2 emissions. Alongside the above applications, the need of increasingly efficient and high-performing energy storage systems is assuming more and more importance [1].

The needs related to the sustainable energy management focus the research activities on the storage systems technologies and their applications. Supercapacitors (SCs) represent an enabling technology introducing advantages both from technical and economic points of view. Thanks to their characteristics, SCs are particular caps able to store a greater amount of electric charge, if compared to the traditional ones [2]. SCs can be charged and discharged almost instantly, guaranteeing high specific power. Besides, the number of charge/discharge cycles are much higher than those of traditional storage systems. SCs find their application in different fields. As a matter of fact, they can be employed in grid-connected applications, in which the combination of SCs and large electrochemical batteries enables the implementation of new grid-services such as the inertia simulation, the power oscillation damping and so on [3]. In particular cases, they are employed as adaptive protection against communication outages in microgrids [4]. Even though the grid-connected applications are manifold, SCs find their main use is in the automotive field. They can be used in hybrid energy storage systems alongside traditional Li-ion batteries [5]-[6] or Fuel Cells [7]. One of the main aspects that cannot be neglected in the study of SC applications is their modelling. Literature shows different approaches that can be summarized into three main areas: electrochemical, thermal and circuital modelling. Electrochemical models are mainly based on the impedance spectroscopy. They are mostly used to investigate the ageing effect due to a cycling use of the SCs [8]. Despite being extremely accurate, an electrochemical approach implies the analysis of several internal parameters such as the equivalent distributed resistance, the time taken by a reactant to diffuse from one side of the SC layer to the other and so on, resulting in very high computational effort. Thermal models, starting from the governing equations of the SCs working principles, are used to detect the temperature distribution during the charging/discharging operations by taking into account several factors such as the current density, the collector and the separator materials [9]. The thermal approach is very useful to estimate the main parameters of a SC, but in most cases it is possible to characterize the SC behaviour only for specific boundary conditions. Besides, the heat conduction model has to be chosen on the base of the construction geometry. For example, the stacked-type capacitors and the rolled-type capacitors, which are the main typologies of commercial SCs, cannot be modelled with the same approach, making the analysis method not very versatile. The most used modelling approach in model-based design of engineering applications is the circuital one.

In its simplest form, the SC equivalent circuit model is composed of a resistor, representing the Equivalent Series Resistance (ESR) of the component, connected in series with a parallel RC branch, representing the capacitance effect of the SC and the self-discharge phenomenon, as proposed in [10]. This kind of equivalent circuit can describe the SC behaviour in the time range of seconds. The applicability of the model could be, for example, the simulation of the converter/control stage considering the PWM frequencies. If a larger time window is needed, further elements can be added to the equivalent circuit to model different dynamics. Focusing on an operating time range from minutes to hours, the so called three-branches model, firstly proposed in [11], is one of the most employed. Main drawbacks of the model presented in [11] are the following ones: the model does not consider the

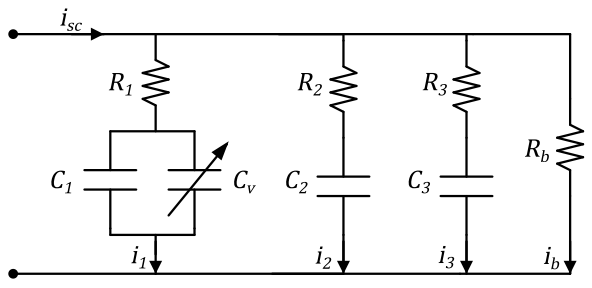

Fig. 1. Three-branches equivalent circuit model.

residual charge phenomenon, and it is validated for a single SC. In most of their applications (e.g. automotive), SCs are connected in series and/or parallel to realize a storage system with the desired rating voltage and power. For this reason, it is essential to verify if the SC model can be easily up-scaled to simulate the behaviour of an entire SCs bank.

This article is based on the authors' previous works [12], [13] and adds the residual charge phenomenon analysis and several experimental tests with different SC bank configurations. It is organized as follows. In Section II the three-branches model of the SC is presented. In Section III the parameter estimation procedure and the test-bench used for the characterization of the Vinatech 2.7 V 100 F SC are fully described. In Section IV, the parameter optimization procedure is explained. In Section V the residual charge phenomenon is highlighted and its implementation in the proposed three-branches model is described. In Section VI the simulation results, obtained in Matlab/Simulink environment, for the single SC and the SCs bank are validated through the comparison with the measured data obtained from the experimental tests carried out, to assess the model accuracy.

II. Three-branches Model Description

To simulate the SCs behaviour in automotive applications, simple scalability and adequate dynamic response are required for the model. The traditional and simplest SC model consists of the series of a capacitor and its internal resistance. Although the simplicity, it is not able to represent the phenomena occurring in a SC over a time window of several hours. To improve the dynamic response of the model, series RC branches can be added. The more branches used, the more accurate the model is, however complexity and computational effort increase. The most widely used model in the literature is the three-branches model, which schematic is depicted in Fig. 1 [11]. It presents a good trade-off between accuracy and complexity.

It features three RC series branches, each one with a different time constant. The first branch, known also as immediate branch, describes the SC instantaneous behaviour. It is composed of a fixed resistor R_1, a fixed capacitor C_1 and a voltage dependent capacitor C_v. The time constant is in the range of seconds. The voltage across the first branch fixed capacitor, v_{C_1} can be expressed as

$$v_{C_1} = v_{sc} - i_1 R_1 \tag{1}$$

where:

- v_{sc} is the voltage at the SC terminal,
- i_1 is the first branch current.

The current in the first branch, considering the voltage dependent capacitor, can be expressed as

$$i_1 = (C_1 + C_v v_{C_1}) \frac{dv_{C_1}}{dt}. \tag{2}$$

The second branch, or delayed branch, consists of a fixed resistor R_2 and a fixed capacitor C_2 and has a time constant of a few minutes. The voltage across the second branch fixed capacitor, v_{C_2}, can be expressed as

$$v_{C_2} = v_{sc} - i_2 R_2 \tag{3}$$

where i_2 is the second branch current expressed as

$$i_2 = C_2 \frac{dv_{C_2}}{dt}. \tag{4}$$

The third branch, also called long-term branch is composed of a fixed resistor R_l and a fixed capacitor C_l and has time constant of hours. The voltage across the third branch fixed capacitor can be expressed as

$$v_{C_3} = v_{sc} - i_3 R_3 \tag{5}$$

where i_3 is the second branch current expressed as

$$i_3 = C_3 \frac{dv_{C_3}}{dt}. \tag{6}$$

In Fig. 1 equivalent circuit, a fourth branch is added to consider the possibility of an external balancing resistor R_b. The total current flowing in the SC terminal can be finally expressed as:

$$i_{sc} = i_1 + i_2 + i_3 + i_b. \tag{7}$$

III. Three-branches Model Parametrization

To parametrize and validate the SC model, an experimental set-up is implemented, it is composed of:

- Vinatech supercapacitors, whose characteristics are reported in Table I;
- a Fluke PM2812 Programmable Power Supply, whose characteristics are reported in Table II, used to charge the SC;
- an Agilent 6060B Single Input Electronic Load, whose characteristics are reported in Table III, used on the discharge phase of the SC;
- a NI 9215 16-Bit Data Acquisition Board (placed in a NI cDAQ 9172 chassis), whose characteristics are reported in Table IV, used to acquire the SC voltage and current waveforms.

Fig. 2 shows a block diagram illustration of the implemented test-bench. The PM1812 and HP6060B are connected to a PC using GPIB, while the CompactRIO system with the NI9215 Analog Input is connected using USB. Both electronic load and programmable power supply are connected in remote sensing operation, so the voltage drop across the leads can be eliminated. The SC voltage is directly acquired using the differential input of the NI9215 module, with 10 kS/s sampling frequency. The obtained samples are then averaged over a 0.1 s

time window. All the experiments were carried out after the calibration of the acquisition board.

To estimate the model parameters, the procedure outlined in [14] is used. The procedure consists of:

1) a constant current charge phase, till the SC reaches its rated voltage,
2) a rest phase, during which the SC is left in open circuit for half an hour,
3) a post-processing phase, during which the SC acquired voltage response is employed for an event recognition analysis.

In order to repeat the test several times, the procedure is automated by creating a virtual instrument in LabView 2016, performing the following tasks:

1) the SC is charged to the desired voltage, using the PM2812 programmable power supply in current mode with a fixed value I_{ch},
2) the power supply is disconnected and the SC is left in open circuit when the SC reaches the desired voltage,
3) the voltage across the SC is acquired continuously for the desired time window,
4) the SC is discharged using the Agilent 6060B electronic load and can be left in short-circuit for the desired amount of time,
5) the acquired voltage is saved into a .xlsx file and exported to Matlab for the parameter estimation procedure.

A Matlab script is implemented to automatically find all the event and to estimate the model parameters as reported in the following paragraphs.

The parameter estimation procedure is performed on several new SCs. Table V summarizes the estimated parameters for four different SCs, as well as the calculated average values.

A. Immediate Branch Parameters

1) Event n. 0: The test starts ($t_0 = 0$) with a fully discharged SC ($V_0 \cong 0$). The current source is switched on going from 0 to $I_{ch} = 5$ A.

2) Event n. 1: The first voltage drop is mainly due to the resistor R_1. The immediate branch fixed resistor value can be estimated as

$$R_1 = \frac{V_1 - V_0}{I_{ch}} \tag{8}$$

where V_1 is the voltage value after the initial voltage drop.

3) Event n. 2: The point in which $V_2 = V_1 + \Delta$ V, with $\Delta V = 50$ mV is found and the elapsed time t_2 is evaluated. The fixed capacitance C_1 can be estimated as

$$C_1 = \frac{I_{ch}\Delta t}{\Delta V} \tag{9}$$

where $\Delta t = t_2 - t_1$.

4) Event n. 3: The point in which $V_3 = V_{max}$ if found and t_3 is evaluated. The current source is switched off ($I_{ch} = 0$).

5) Event n. 4: The voltage V_4 at time $t_4 = t_3 + t_{sd}$ is evaluated. t_{sd} is the shut-down time of the current source. The voltage dependent capacitance C_v can be estimated as

$$C_v = \frac{2}{V_4} \cdot \left(\frac{I_{ch} \cdot (t_4 - t_1)}{V_4} - C_1 \right). \tag{10}$$

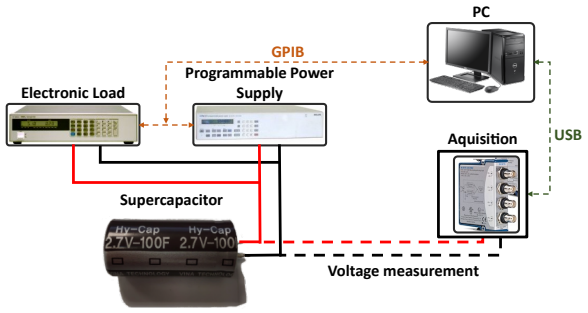

Fig. 2. Block diagram of the experimental set-up.

TABLE I
SUPERCAPACITOR DATA-SHEET SPECIFICATIONS

SPECIFICATION	UNIT	VALUE
Rated voltage	V	2.7
Rated capacitance	F	100
AC impedance (1 kHz)	mΩ	6
DC resistance	mΩ	10
Maximum current	A	65
Leakage current	mA	0.2
Stored energy	J	364.5

B. Delayed Branch Parameters

1) Event n.5: The point in which $V_5 = V_4 - \Delta V$ is found. $\Delta t = t_5 - t_4$ is evaluated. The delayed branch fixed resistance can be estimated as

$$R_2 = \frac{\left(V_4 - \frac{\Delta V}{2}\right) \cdot \Delta t}{\left[C_1 + C_v \left(V_4 - \frac{\Delta V}{2}\right)\right]}. \tag{11}$$

2) Event n.6: The point at the time $t_6 = t_5 + 3R_2C_2$ is found. Supposing a typical time constant of 100 seconds, V_6 is evaluated.

$$C_2 = I_{ch} \cdot \frac{t_4 - t_1}{V_6} - \left(C_1 + \frac{C_v}{2} \cdot V_6\right). \tag{12}$$

C. Long-term Branch Parameters

1) Event n.7: The point in which $V_7 = V_6 - \Delta V$ is found and $\Delta t = t_7 - t_6$ is evaluated. The fixed resistance of the long-term branch can be estimated as

$$R_3 = \frac{\left(V_6 - \frac{\Delta V}{2}\right) \Delta t}{(C_1 + C_v)\left(V_6 - \frac{\Delta V}{2}\right) \Delta V}. \tag{13}$$

2) Event n.8: At the end of the test $t_8 = 30$ min, V_8 is evaluated. The long-term capacitance can be estimated as

$$C_3 = I_{ch} \cdot \frac{t_4 - t_1}{V_8} - \left(C_1 + \frac{C_v}{2} \cdot V_8\right) - C_2. \tag{14}$$

TABLE II
PM2818 PROGRAMMABLE POWER SUPPLY SPECIFICATIONS

	Current	Voltage
Ratings	$0 \div 10$ A	$0 \div 60$ V
Accuracy	$\pm(0.1\% + 25)$ mA	$\pm(0.04\% + 20)$ mV

TABLE III
HP 6060B ELECTRONIC LOAD SPECIFICATIONS

	Current	Voltage
Ratings	$0 \div 60$ A	$3 \div 60$ V
Accuracy	$\pm(0.1\% + 75)$ mA	$\pm(0.1\% + 50)$ mV

TABLE IV
NI 9215 ANALOG INPUT MODULE SPECIFICATIONS

Signal levels	± 10 V
Sample rate	100 kS/s
Accuracy	$\pm(0.02\% + 1.46)$ mV
Resolution	16-bit

TABLE V
SUPERCAPACITOR THREE-BRANCHES MODEL PARAMETERS

Parameter	Unit	SC_1	SC_2	SC_3	SC_4	Average
R_1	mΩ	7.01	7.03	7.00	6.99	7.00
R_2	Ω	4.54	2.19	2.07	1.62	1.96
R_3	Ω	40.96	29.07	28.59	12.73	23.46
C_1	F	73.26	75.09	76.74	86.00	79.28
C_v	F/V	23.90	22.57	22.75	11.98	19.09
C_2	F	45.91	66.12	67.51	58.14	63.92
C_3	F	58.04	64.47	64.47	61.06	63.33

IV. PARAMETER OPTIMIZATION

The parameters estimated with the procedure described in Section III can be finely tuned by using an appropriate optimization algorithm. A Nonlinear Least Squares Method (NLSM) is employed. Its mathematical formulation is provided in (15)

$$\min F(p) \quad \text{subject to} \begin{cases} C_{leq}(p) \leq 0 \\ C_{eq}(p) = 0 \\ A \times p \leq B \\ A_{eq} \times p = B_{eq} \\ lb \leq p \leq ub \end{cases} \tag{15}$$

in which $F(p)$ is the objective function, p is the optimization vector, composed by the variables $R_1, R_2, R_3, C_1, C_v, C_2, C_3$, C_{leq} and C_{eq} are the nonlinear inequality and equality constraints, A and B are the linear inequality constraints, A_{eq} and B_{eq} are the linear equality constraints, lb and ub are the lower and upper bounds on p. The simulation model is implemented in Matlab/Simulink environment, by using the Simscape Electrical Toolbox to realize the schematic reported in Fig. 4. The parameter average values (Table V) are set

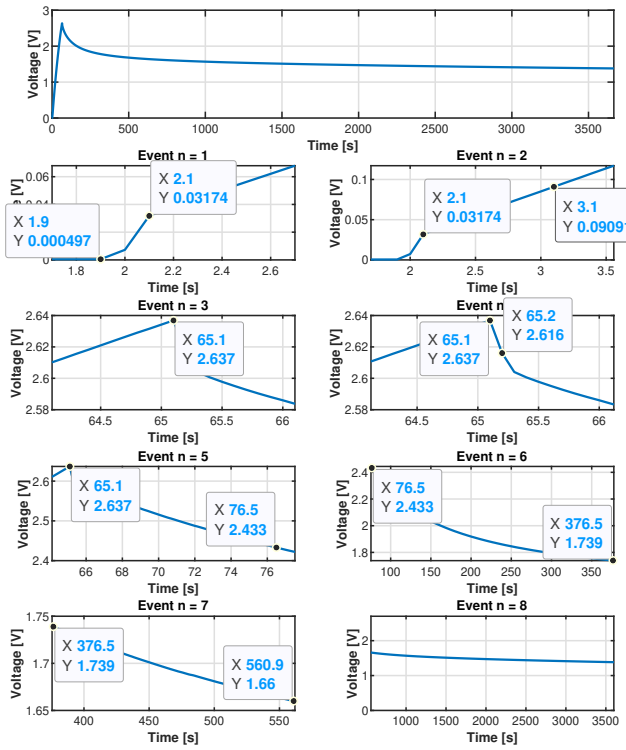

Fig. 3. Event recognition for SC parameters estimation.

as initial guesses for p, thereby improving the convergence chances of the method. The optimization algorithm starts by simulating the aforementioned Simulink model, then from the comparison between the model output and the measured experiment data, the cost function is evaluated in p and the parameters are updated. The procedure is iterated until a local minimum on the residuals is achieved. The resulting optimized parameters are summarized in Table VI.

The results of the optimization procedure are highlighted in Fig. 5, where the simulated waveforms are compared to the experimental dataset. The accuracy of the model is evaluated through the following indices.

Instantaneous error:

$$Err(t_i) = A(t_i) - S(t_i), \tag{16}$$

where:

- $A(t_i)$ is the experimental value at the considered instant t_i,
- $S(t_i)$ is the simulated value at the considered instant t_i.

Average error:

$$Err_{mean} = \frac{\sum_{i=1}^{N} [A(t_i) - S(t_i)]}{N}, \tag{17}$$

where N is the number of samples of the experimental and simulated data.

Maximum error

$$Err_{max} = \max(|Err(t_i)|). \tag{18}$$

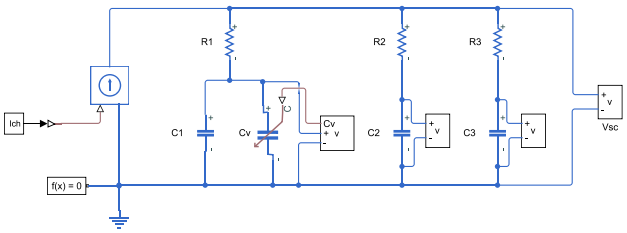

Fig. 4. Simulink schematic of the three-branches model.

TABLE VI
OPTIMIZED PARAMTERS FOR THE SC THREE-BRANCHES MODEL

R_1 (mΩ)	R_2 (Ω)	R_3 (Ω)	C_1 (F)	C_v (F/V)	C_2 (F)	C_3 (F)
13.2	2.02	28.2	76.5	22.3	69.0	64.7

Fig. 5 (a) shows the simulation results using the estimated parameters, superimposed to the experimental SC voltage, and the instantaneous error trend. Before the optimization process, the maximum error is 186 mV and the mean error is 56.9 mV.

Fig. 5 (b) shows the simulation results with the optimized parameters, superimposed to the experimental SC voltage, and the instantaneous error trend. After the optimization process, the maximum error is 92.2 mV and the mean error is 1.7 mV, effectively increasing the accuracy of the model.

As further evidence of the model accuracy, the simulated voltage response with the optimized parameters is compared with several different experimental datasets in Fig. 6. It can be noticed that the model fits quite well the experimental results in all cases, with the worst case maximum and mean error respectively equal to 112 mV and 20 mV.

V. RESIDUAL CHARGE PHENOMENON

The model presented in [14] does not consider the residual charge phenomenon.The SCs can store energy for a very long period (e.g. weeks). For this reason, they always present a residual charge, or in other word, an initial condition (IC) other than zero. This residual charge has a great influence on the SC dynamic behaviour.

The residual charge phenomenon also affects the parameters estimation procedure. For a proper estimation, it is essential to have the same initial conditions for both the model and the experimental set-up. The SC initial conditions are practically not measurable. For this reason, the parameters estimation procedure should be always applied to a brand new SC (or, at least, left unloaded for several weeks).

Fig. 7 shows the residual charge effect on the SC voltage response. The SC is charged to the rated voltage and then totally discharged thanks to the electronic load. Then it is left short-circuited for different resting periods and finally charged again to the rated voltage. The green curve depicts the voltage response for a brand new SC. The blue, orange, yellow and purple curves are obtained by leaving the SC short-circuited respectively for one minute, one day, one week and two weeks respectively. Two main effects can be observed:

TABLE VII
ESTIMATED INITIAL CONDITIONS FOR DIFFERENT SC RESTING PERIOD

	V_{C_1} (V)	V_{C_2} (V)	V_{C_3} (V)
One minute	0.1385	2.6990	0.0348
One Week	0.1170	2.1830	0
Two weeks	0.9852	0.9313	0

1) the higher the residual charge, the shorter the charging time, as can be seen from the enlargement shown in the figure; 2) the higher the residual charge, the less pronounced the charge redistribution effect is during the resting phase.

The residual charge effect can be considered into the three-branches model by setting an IC for each capacitor composing it. Since the residual charge cannot be directly measured, the ICs are estimated by setting-up a new optimization problem.

The new experimental dataset is obtained with the following procedure:

1) charge the SC with a constant current, up to its rated voltage;
2) totally discharge the SC;
3) repeat point 1 and 2 ten times;
4) short-circuit the SC and wait for a defined rest period;
5) perform a new charge/discharge cycle and acquire the SC voltage.

The above procedure is repeated for different rest periods, in particular one minute (corresponding to high residual charge), one week (medium residual charge) and two weeks (low residual charge). The estimated initial voltage for the capacitors C_1, C_2 and C_3 are reported in Table VII. The branch with the strongest influence on the SC voltage dynamic is the second one (delayed branch) whose initial voltage goes from 2.7 V (practically the charge voltage of the SC) in the case of one minute rest to 0.9 V in the case of two weeks rest.

Fig. 8 shows the simulation results after the estimation of the ICs for three different resting periods, the instantaneous error trend and reports the maximum and mean error values. The orange curves in Fig. 8 (a), (b), (c) report the simulation results, with initial conditions equal to zero. The blue curves depict the SC experimental voltage response after (a) one minute rest, (b) 1 week rest and (c) two weeks rest. The yellow curves show the simulation results considering the estimated initial conditions. It can be noticed that the accuracy of the model is greatly improved, obtaining errors comparable to the case of the simulation of brand new SC.

VI. MODEL VALIDATION OF SUPERCAPACITORS BANKS

A shortcoming of many of the literature articles, such as [14]-[17], is to validate the model for a single SC unit. In real cases, SCs are assembled in banks, with multiple units connected in series and/or parallel to increase the overall voltage and current ratings.

The three-branches model can be easily updated to simulate the performances of a SCs bank considering the number of series N_s and parallel N_p connected components. Specifically,

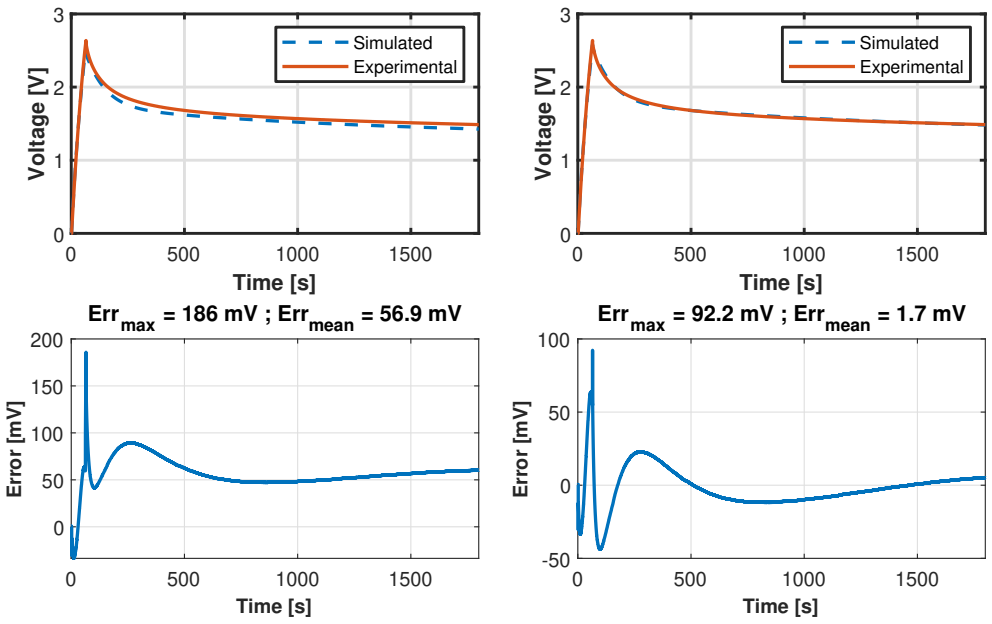

Fig. 5. Simulated vs Experimental SC voltage response,instantaneous error trend, maximum and mean error values: (a) before the parameter optimization process; (b) after the parameter optimization process.

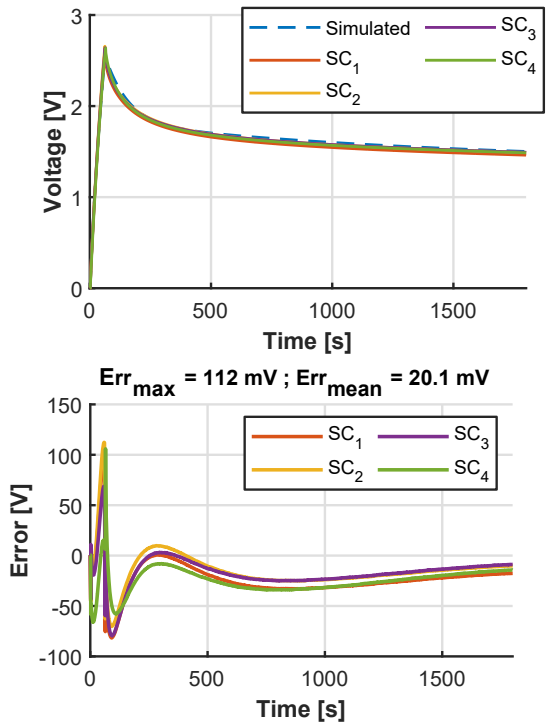

Fig. 6. Simulated voltage response using the optimized parameters compared to the experimental voltage response of different SCs and instantaneous error trend with maximum and mean values.

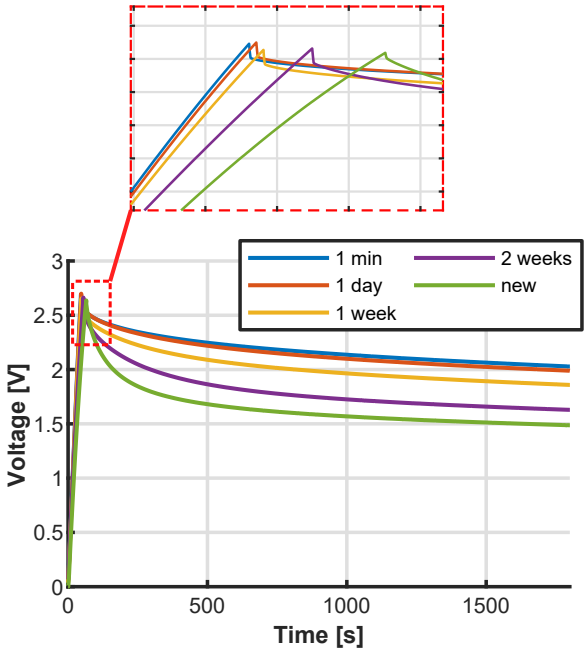

Fig. 7. Residual charge effect on the SC voltage response for different SC resting period (different values of the residual charge).

the bank voltage and current are obtained starting from the single SC voltage and current equations:

$$v_{bank} = N_s \cdot v_{sc}, \tag{19}$$

$$i_{bank} = N_p \cdot (i_1 + i_2 + i_3 + i_b). \tag{20}$$

It is worth noting that this approach assumes that all SCs are identical. In practice, they may have subtly different parameters. To investigate whether this approximation is acceptable, the model is validated for different SC bank configurations: 1) single SCs bank module, 2) two parallel connected SC bank modules, 3) two series connected SC bank modules.

The SC bank module characteristics [18] are reported in Table VIII. The SC bank modules, shown in Fig. 9, are composed of 24 units in series, each with a 510 Ω parallel

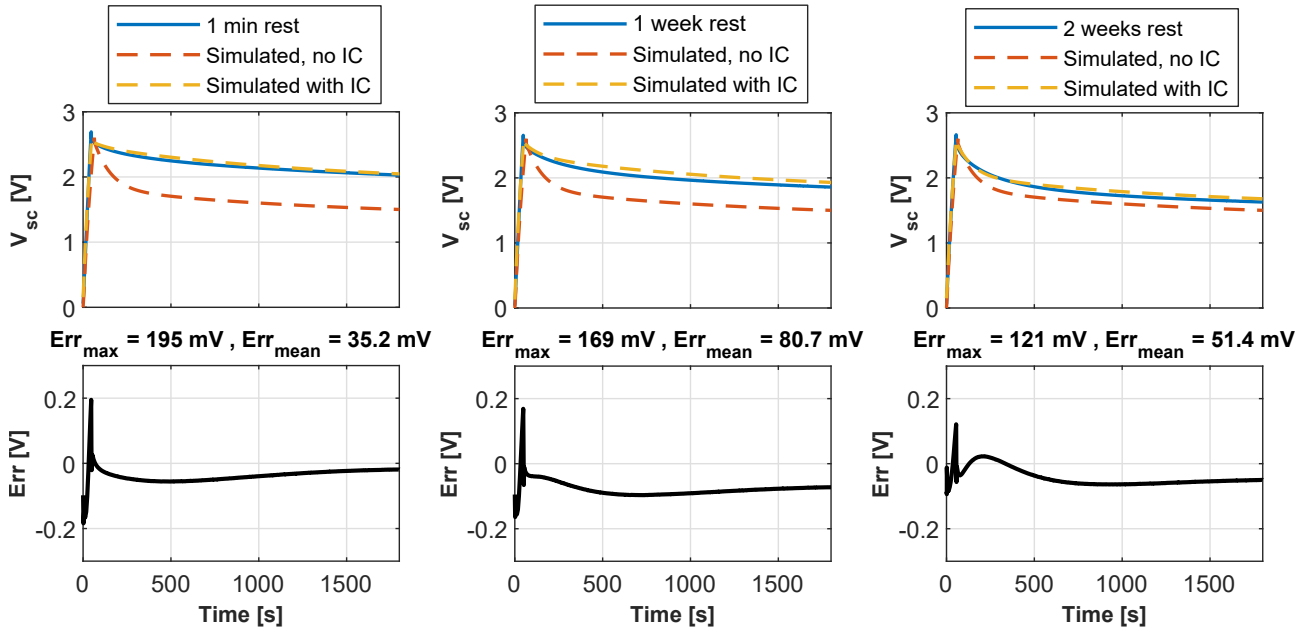

Fig. 8. Initial condition effects on the model accuracy for a SC after: (a) one minute rest (high residual charge); (b) one week rest (medium residual charge); (c) two weeks rest (low residual charge).

TABLE VIII
SUPERCAPACITOR BANK SPECIFICATIONS

SPECIFICATION	UNIT	VALUE
Series component N_s	-	24
Parallel components N_p	-	1
Nominal capacitance	F	4.17
Balancing resistor R_b	Ω	510
Nominal voltage	V	60
Nominal current	A	20
Maximum current	A	57

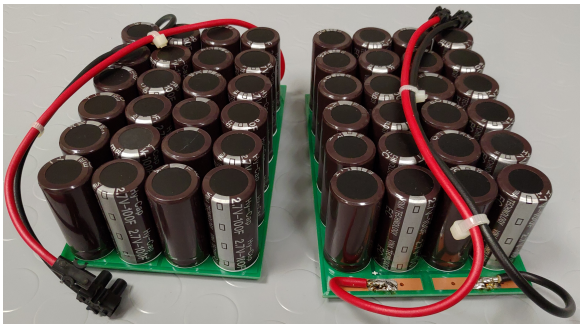

Fig. 9. SC banks used for experimental validation.

resistor for self-discharge and passive balancing.

To validate the model, two different experimental tests for each bank configuration are carried out.

The first test is similar to the one used for the parameter estimation. The SCs bank is charged up to 48 V with 2 A constant current. Fig. 10 shows the SCs bank voltage superimposed to the simulation results, the SCs bank current, and the instantaneous error trend for (a) the single SCs configuration (b) the parallel SC banks configuration, (c) the series SC banks configuration. Although the simplified approach of considering all components identical, the model estimates the SCs bank terminal voltage with sufficient accuracy. The mean error ranges from 0.372 V for the single SCs bank to 1.28 V for the parallel SC banks and the maximum error is 5.07 V (8.45% of the maximum observed voltage) for the series SC banks.

The second test is the Hybrid Pulse Power Characterization (HPPC) [19] test. It consists in alternately apply a charge and discharge current to the device under test, with a rest period in between. The HPPC is chosen because it can be considered as a simple approximation of the SCs bank behaviour in automotive applications.

Fig. 11 shows the voltage, current and error trends for the three different SC bank configurations. Considering Fig. 11 (a), in the first phase, from $t = 0$ s to $t = 120$ s, the SCs bank is charged with a constant current up to 48 V. In the second phase, from $t = 120$ to $t = 160$ s, the SCs bank is charged with a constant voltage equal to 48 V until the current falls below 0.4 A. In the third phase, the HPPC test begins with the following settings.

- Charge current: 2 A;
- charge pulse duration: 10 s;
- rest period: 10 s;
- discharge current 3 A;
- discharge pulse duration: 10.

The HPPC test is repeated until the SCs bank voltage reaches half of the initial value (i.e. 24 V). The tests on the other SC bank configurations are performed adjusting the charge, rest and discharge duration, with the same charging and discharging current. For the series SC banks, the maximum charging voltage is set to 60 V, that is the maximum allowable voltage for the employed test-bench. All three

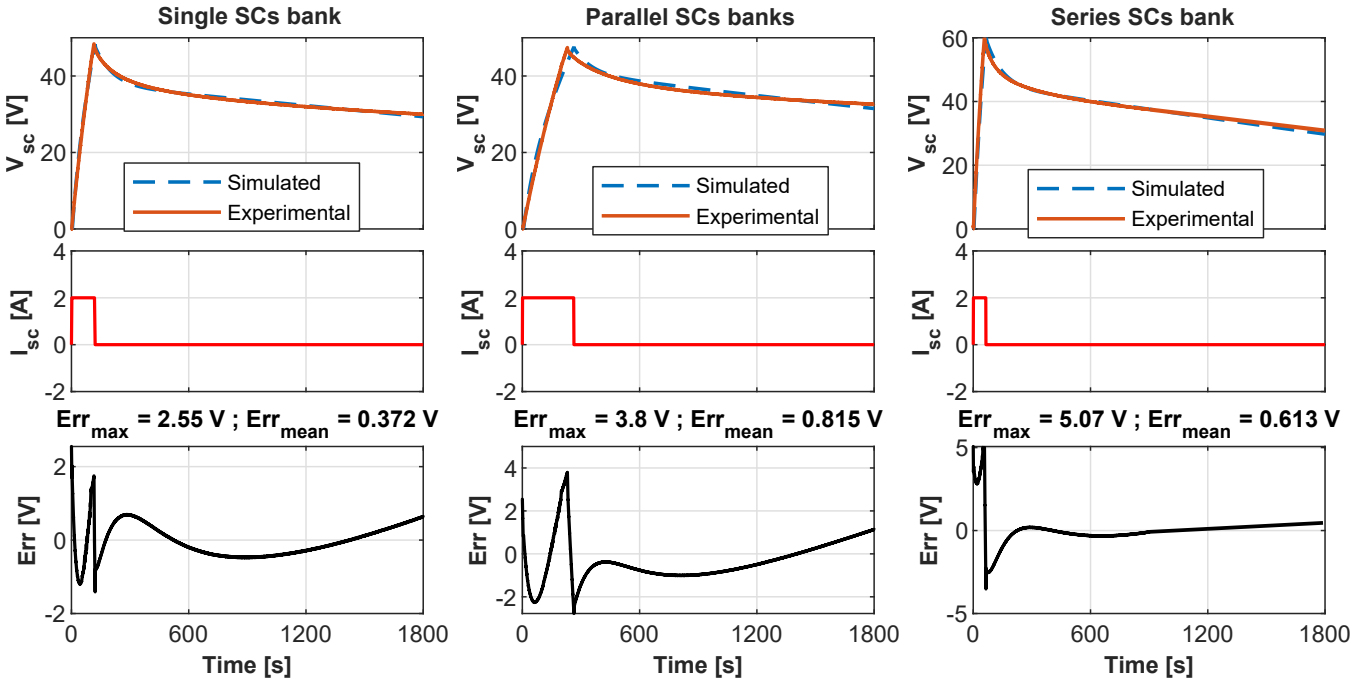

Fig. 10. Constant current charge results with voltage, current and error trend for different banks configurations: (a) single SCs bank; (b) parallel SCs banks; (c) series SCS banks.

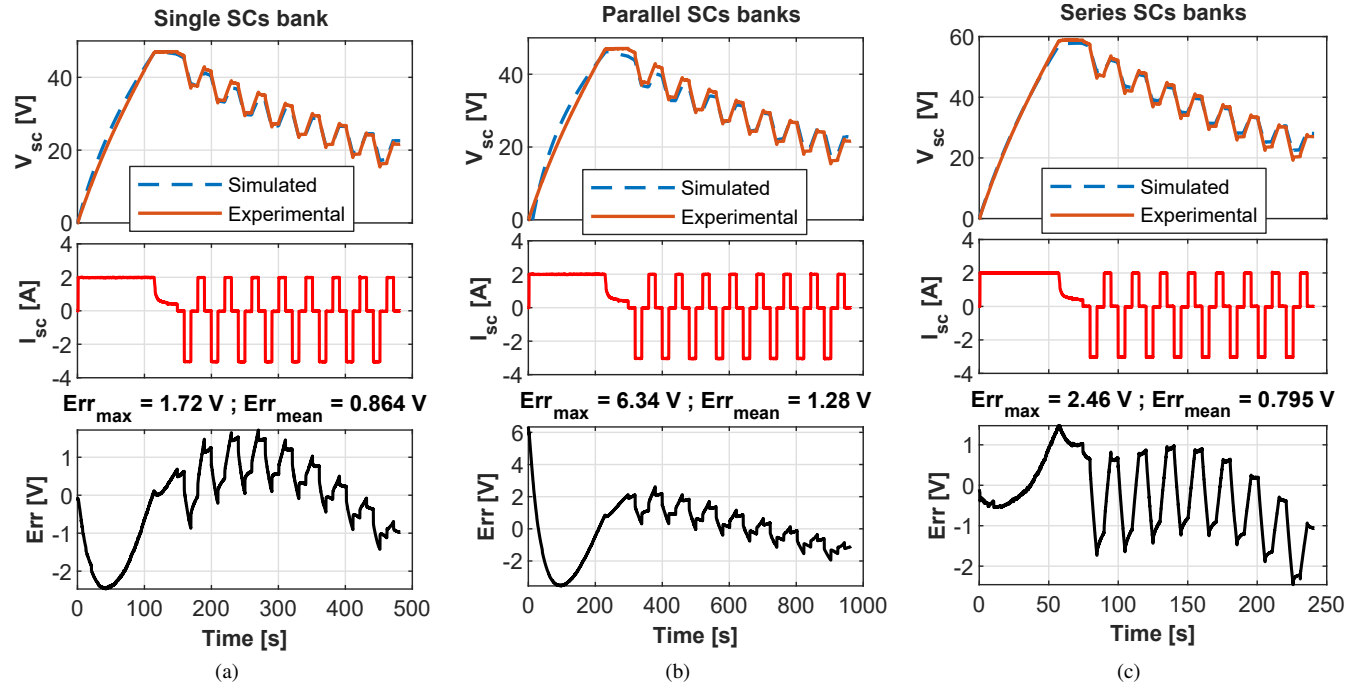

Fig. 11. HPPC test results with voltage, current and error trend for different banks configurations: (a) single SCs bank; (b) parallel SCs banks; (c) series SCS banks.

configurations are properly simulated, with a mean error of 0.864 V for the single SCs bank, 1.28 V for the parallel SC banks and 0.795 V for the series SC banks.

VII. Conclusion

In this article, an improved SC three-branches equivalent circuit model has been presented along with a parameter estimation and optimization procedure. Most of the SC models proposed in literature are validated only for a single cell, while the one presented in the article is scalable and suitable for the simulation of an entire bank. The proposed model has been experimentally validated and compared with simulations performed in Matlab/Simulink environment. The average error observed on a single SC is equal to about 1% of the maximum cell voltage (2.7 V), while it is equal to 1.7% for a SC bank (50 V), demonstrating its good scalability and accuracy. In addition, the proposed model takes into account the residual charge phenomenon. The latter is associated with the diffusion of SC residual charges during charge, discharge and rest phases and it has an important effect on the dynamic response of the SC, as demonstrated in the article. With the proposed improvement, it is possible to minimize the error due to this effect by taking into account the SC initial condition.

Acknowledgment

This work was financially supported by PON R&I 2015-2020 "Propulsione e Sistemi Ibridi per velivoli ad ala fissa e rotante – PROSIB", CUP no:B66C18000290005, by H2020-ECSEL-2017-1-IA-two-stage, by "first and european sic eight-inches pilot line-REACTION", by Prin 2017- Settore/Ambito di intervento: PE7 linea C - Advanced power-trains and -systems for full electric aircrafts, by PON R&I 2014-2020 - AIM (Attraction and International Mobility), project AIM1851228-1 and by ARS01_00459-PRJ-0052 ADAS+ "Sviluppo di tecnologie e sistemi avanzati per la sicurezza dell'auto mediante piattaforme ADAS".

References

[1] M. Aneke and M. Wang, "Energy storage technologies and real life applications - a state of the art review," *Applied Energy*, vol. 179, pp. 350–377, 2016.

[2] E. Chemali, M. Preindl, P. Malysz, and A. Emadi, "Electrochemical and electrostatic energy storage and management systems for electric drive vehicles: State-of-the-art review and future trends," *IEEE Journal of Emerging and Selected Topics in Power Electronics*, vol. 4, no. 3, pp. 1117–1134, 2016.

[3] J. Rocabert, R. Capó-Misut, R. S. Muñoz-Aguilar, J. I. Candela, and P. Rodriguez, "Control of energy storage system integrating electrochemical batteries and supercapacitors for grid-connected applications," *IEEE Transactions on Industry Applications*, vol. 55, no. 2, pp. 1853–1862, 2019.

[4] H. F. Habib, M. E. Hariri, A. Elsayed, and O. A. Mohammed, "Utilization of supercapacitors in protection schemes for resiliency against communication outages: A case study on size and cost optimization," *IEEE Transactions on Industry Applications*, vol. 54, no. 4, pp. 3153–3164, 2018.

[5] A. Mamun, Z. Liu, D. M. Rizzo, and S. Onori, "An integrated design and control optimization framework for hybrid military vehicle using lithium-ion battery and supercapacitor as energy storage devices," *IEEE Transactions on Transportation Electrification*, vol. 5, no. 1, pp. 239–251, 2019.

[6] M. Passalacqua, D. Lanzarotto, M. Repetto, L. Vaccaro, A. Bonfiglio, and M. Marchesoni, "Fuel economy and ems for a series hybrid vehicle based on supercapacitor storage," *IEEE Transactions on Power Electronics*, vol. 34, no. 10, pp. 9966–9977, 2019.

[7] J. Chen and Q. Song, "A decentralized dynamic load power allocation strategy for fuel cell/supercapacitor-based apu of large more electric vehicles," *IEEE Transactions on Industrial Electronics*, vol. 66, no. 2, pp. 865–875, 2019.

[8] H. Ahmad, W. Y. Wan, and D. Isa, "Modeling the ageing effect of cycling using a supercapacitor-module under high temperature with electrochemical impedance spectroscopy test," *IEEE Transactions on Reliability*, vol. 68, no. 1, pp. 109–121, 2019.

[9] Y. Li, S. Wang, M. Zheng, and J. Liu, "Thermal behavior analysis of stacked-type supercapacitors with different cell structures," *CSEE Journal of Power and Energy Systems*, vol. 4, no. 1, pp. 112–120, 2018.

[10] P. Sharma and T. Bhatti, "A review on electrochemical double-layer capacitors," *Energy Conversion and Management*, vol. 51, no. 12, pp. 2901–2912, 2010. [Online]. Available: https://www.sciencedirect.com/science/article/pii/S0196890410002438

[11] L. Zubieta and R. Bonert, "Characterization of double-layer capacitors (dlcs) for power electronics applications," in *Conference Record of 1998 IEEE Industry Applications Conference. Thirty-Third IAS Annual Meeting (Cat. No.98CH36242)*, vol. 2, 1998, pp. 1149–1154.

[12] V. Castiglia, N. Campagna, C. Spataro, C. Nevoloso, F. Viola, and R. Miceli, "Modelling, simulation and characterization of a supercapacitor," in *2020 IEEE 20th Mediterranean Electrotechnical Conference (MELECON)*, 2020, pp. 46–51.

[13] V. Castiglia, N. Campagna, A. O. Di Tommaso, R. Miceli, F. Pellitteri, C. Puccio, and F. Viola, "Modelling, simulation and characterization of a supercapacitor in automotive applications," in *2020 Fifteenth International Conference on Ecological Vehicles and Renewable Energies (EVER)*, 2020, pp. 1–6.

[14] L. Zubieta and R. Bonert, "Characterization of double-layer capacitors for power electronics applications," *IEEE Transactions on Industry Applications*, vol. 36, no. 1, pp. 199–205, 2000.

[15] D. Xu, L. Zhang, B. Wang, and G. Ma, "Modeling of supercapacitor behavior with an improved two-branch equivalent circuit," *IEEE Access*, vol. 7, pp. 26 379–26 390, 2019.

[16] D. Torregrossa, M. Bahramipanah, E. Namor, R. Cherkaoui, and M. Paolone, "Improvement of dynamic modeling of supercapacitor by residual charge effect estimation," *IEEE Transactions on Industrial Electronics*, vol. 61, no. 3, pp. 1345–1354, 2014.

[17] C. Quintáns, R. Iglesias, A. Lago, J. M. Acevedo, and C. Martinez-Penalver, "Methodology to obtain the voltage-dependent parameters of a fourth-order supercapacitor model with the transient response to current pulses," *IEEE Transactions on Power Electronics*, vol. 32, no. 5, pp. 3868–3878, 2017.

[18] H2planet. [Online]. Available: https://www.h2planet.eu/it/detail/HyCaps

[19] J. P. Christopherson, *Battery Test Manual For Electric Vehicles*, Idaho National Laboratory.